HHS Public Access

Author manuscript

Cell Host Microbe. Author manuscript; available in PMC 2017 June 30.

Published in final edited form as:

Cell Host Microbe. 2016 September 14; 20(3): 318–328. doi:10.1016/j.chom.2016.08.001.

Mammalian Innate Immune Response to a *Leishmania*-Resident RNA Virus Increases Macrophage Survival to Promote Parasite Persistence

Remzi Onur Eren[1], **Marta Reverte**[1], **Matteo Rossi**[1], **Mary-Anne Hartley**[1], **Patrik Castiglioni**[1], **Florence Prevel**[1], **Ricardo Martin**[1], **Chantal Desponds**[1], **Lon-Fye Lye**[2], **Stefan K. Drexler**[1,4], **Walter Reith**[3], **Stephen M. Beverley**[2], **Catherine Ronet**[1], and **Nicolas Fasel**[1,5,*]

[1]Department of Biochemistry, University of Lausanne, 1066 Epalinges, Switzerland [2]Department of Molecular Microbiology, School of Medicine, Washington University, St. Louis, MO 63110, USA [3]Department of Pathology and Immunology, University of Geneva, 1211 Geneva, Switzerland

SUMMARY

Some strains of the protozoan parasite *Leishmania guyanensis* (L.g) harbor a viral endosymbiont called *Leishmania* RNA virus 1 (LRV1). LRV1 recognition by TLR-3 increases parasite burden and lesion swelling in vivo. However, the mechanisms by which anti-viral innate immune responses affect parasitic infection are largely unknown. Upon investigating the mammalian host's response to LRV1, we found that miR-155 was singularly and strongly upregulated in macrophages infected with LRV1+ L.g when compared to LRV1 − L.g. LRV1-driven miR-155 expression was dependent on TLR-3/TRIF signaling. Furthermore, LRV1-induced TLR-3 activation promoted parasite persistence by enhancing macrophage survival through Akt activation in a manner partially dependent on miR-155. Pharmacological inhibition of Akt resulted in a decrease in LRV1-mediated macrophage survival and consequently decreased parasite persistence. Consistent with these data, miR-155-deficient mice showed a drastic decrease in LRV1-induced disease severity, and lesional macrophages from these mice displayed reduced levels of Akt phosphorylation.

Graphical Abstract

[*]Correspondence: nicolas.fasel@unil.ch.
[4]Present address: Biozentrum, University of Basel, 4056 Basel, Switzerland
[5]Lead Contact

AUTHOR CONTRIBUTIONS

Conceptualization, R.O.E. and N.F.; Methodology, R.O.E. and N.F.; Investigation, M. Reverte, M. Rossi, M.-A.H., P.C., F.P., R.M., C.H., S.K.D., C.R., R.O.E., and N.F.; Resources, L.-F.L., W.R., and S.M.B.; Writing – Original Draft, R.O.E. and N.F.; Writing – Review & Editing, W.R., S.M.B., C.R., R.O.E., and N.F.; Funding Acquisition, M.-A.H., C.R., S.M.B., and N.F.

ACCESSION NUMBERS

The ArrayExpress accession number for the microRNA microarray is E-MTAB-4413.

SUPPLEMENTAL INFORMATION

Supplemental Information includes Figures S1–S6, Table S1, and Supplemental Experimental Procedures and can be found with this article online at http://dx.doi.org/10.1016/j.chom.2016.08.001.

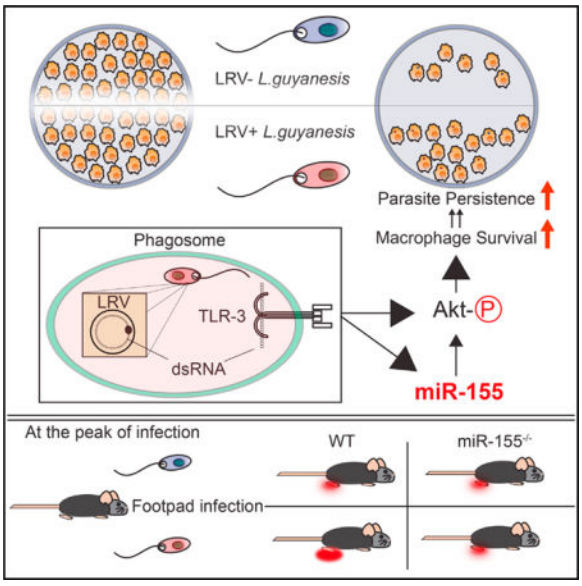

INTRODUCTION

Macrophages are host cells for several obligate intracellular protozoan parasites such as *Leishmania spp.*, *Trypanosoma cruzi*, and *Toxoplasma gondii* (Sacks and Sher, 2002). Upon infection, macrophages shape the early phases of immunity by sensing pathogen-associated molecular patterns (PAMPs) through pathogen recognition receptors (PRRs). The family of Toll-like receptors (TLRs) is one of the most intensively studied classes of PRRs. The engagement of TLRs with their cognate ligands leads to a cascade of events including the recruitment of various adaptor molecules such as myeloid differentiation primary response gene 88 (MyD88), MyD88 adaptor-like, TIR-domain-containing adaptor-inducing IFN-β(TRIF), and the TRIF-related adaptor molecule. The MyD88 adaptor protein is involved in the signaling of all TLRs except the double-stranded RNA (dsRNA) receptor TLR-3, which exclusively recruits TRIF. Both MyD88-dependent and -independent TLR pathways transduce signals through conserved inflammatory signaling pathways, inducing Interleukin-6 (IL-6) and tumor necrosis factor-α (TNF-α) secretion. TLR stimulation also promotes the activation of phosphatidylinositol 3-kinase (PI3K)/Akt. In addition to these pathways, TRIF-dependent TLR signaling induces the phosphorylation of interferon response element 3 (IRF-3), leading to the transcription of IFN-β (Rakoff-Nahoum and Medzhitov, 2009).

TLR activation of innate cells is involved in the development of parasiticidal immunity via the presentation of parasitic antigens to T cells (Iwasaki and Medzhitov, 2004). Antigen-activated $CD4^+$ T cells are a major source of IFN-γ, which is a key mediator of anti-*Leishmania* effector genes in macrophages (Bogdan et al., 2000). Excessive TLR simulation, however, can be detrimental to the host in chronic infectious diseases, leading to progressive tissue damage and fatal systemic disorders. For example, TLR-3 recognition of an endosymbiotic dsRNA virus within *Leishmania guyanensis* (L.g) increases the virulence of

the virus's microbial host and induces a hyper-inflammatory response by exploiting the innate recognition of *Leishmania*'s mammalian host (Ives et al., 2011).

In addition to initiating inflammation and adaptive immunity, TLRs are known to be involved in macrophage survival (Lombardo et al., 2007). Certain bacterial species hinder TLR-4-mediated cell-survival factors to induce macrophage apoptosis, proposing a mechanism for bacterial immune evasion (Hsu et al., 2004; Park et al., 2005). Several viral species are reported to extend host cell viability by inducing the PI3K/Akt signaling pathway to achieve latent and/or chronic infection (Cooray, 2004). Similarly, intracellular protozoan parasites can promote host cell survival by activating pro-survival signaling pathways or by interrupting host cell apoptotic machinery (Heussler et al., 2001). For example, infection of a murine macrophage cell line with *Leishmania spp.* induces PI3K/Akt signaling and grants protection against apoptosis (Ruhland et al., 2007). Taken together, the subtle equilibrium between the death and survival of innate cells has a determining impact on the outcome of microbial infections.

Akt, a member of the protein kinase B family, is a serine threonine kinase that regulates numerous substrates involved in cell survival, cellular growth, and metabolism. For instance, TLR-3-induced endogenous phosphorylation of Akt in primary murine macrophages leads to the degradation of Forkhead box O3 (Foxo3a), a transcription factor that regulates genes involved in cell death (Litvak et al., 2012). Furthermore, Akt positively regulates the mammalian target of rapamaycin 1 (mTOR1), which plays a key role in cell survival and growth by modulating mRNA translation and many cellular processes in innate cells (Weichhart et al., 2015). The activating serine 2448 phosphorylation of mTOR1 by Akt leads to the phosphorylation of ribosomal protein S6 kinase (S6K), which promotes mRNA translation (Huang and Houghton, 2003).

Another important component of TLR stimulation is the expression of small non-coding RNAs, named microRNAs, which regulate genes at the post-transcriptional level, culminating in the degradation of the transcript or the inhibition of translation (Valencia-Sanchez et al., 2006). In macrophages, mi-croRNA-155 (miR-155) is the only microRNA that is significantly upregulated in response to polyinosinic:polycytidylic acid (poly I:C), a synthetic dsRNA ligand for TLR-3 (O'Connell et al., 2007). MiR-155 is also classified as an oncogenic microRNA. The overexpression of miR-155 in mice causes a myeloid proliferative disorder, which is at least partially due to Akt-mediated cell survival and proliferation (O'Connell et al., 2008). This indicates the oncogenic potential of a TLR-induced microRNA.

In this study, we asked which microRNAs were modulated in macrophages in the presence of L.g endosymbiont *Leishmania* RNA virus 1 (LRV1), and investigated how and by which mechanism(s) LRV1 contributed to increased pathology.

RESULTS

MiR-155 Is the Uniquely Expressed MicroRNA due to LRV1/TLR-3/TRIF Signaling

To determine the impact of LRV1 on the miRNA expression profile, murine bone-marrow macrophages (BMMs) were incubated with LRV1+ L.g or LRV1 − L.g parasites for 10 hr. A miRNA microarray analysis was then performed on total RNA. Out of 1,179 miRNAs, miR-155 was the only miRNA significantly upregulated by LRV1+ L.g infection in comparison to LRV − L.g (Figure 1A). To verify this result, isolated RNA from LRV1+ L.g- or LRV1 − L.g-infected macrophages was reverse transcribed into complementary DNA (cDNA) using a stem-loop primer approach (Hurley et al., 2012). cDNAs were then used to quantify mature miR-155 by real-time PCR (RT-PCR). Consistent with the microRNA microarray data, miR-155 was drastically upregulated in response to poly I:C treatment and LRV1+ L.g infection (Figure 1B). These findings demonstrated that the dsRNA endosymbiont within L.g altered the miRNAome profile of host macrophages and induced the expression of miR-155.

MiR-155 is located in the third exon of the non-protein-coding B cell-integrated cluster (*BIC*) gene (Tam, 2001). To examine the kinetics of miR-155 induction in BMMs following various stimuli, the expression of both *BIC* mRNA and the mature form of miR-155 was monitored for 24 hr post-infection using RT-PCR. In the presence of LRV1 or poly I:C, miR-155 and the *BIC* gene were detected after 2 hr, with a peak at 10 hr post-infection (Figures 1C and 1D). MiR-155 expression stabilized after 10 hr post-incubation, while the transcript level of *BIC* was strongly downregulated in macrophages incubated with LRV1+ L.g and poly I:C after 24 hr (Figures 1C and 1D). Upon LRV1 − L.g infection, *BIC* remained almost undetectable during the 24 hr time course (Figure 1D). In *miR-155*$^{-/-}$ deficient mice, a β-galactosidase reporter gene replaces the third exon of *BIC*, allowing the measurement of *BIC* promoter activity (Thai et al., 2007). LRV1+ L.g- and LRV1 − L.g-infected *miR-155*$^{-/-}$ BMMs were lysed, and cell lysates were tested for β-galactosidase by immunoblotting (Figure 1E). We observed that the β-galactosidase level peaked after 10 hr incubation with LRV1+ L.g or poly I:C. Comparatively, LRV1 − L.g infection induced residual β-galactosidase expression (Figure 1E).

The LRV1 dsRNA genome is an agonist of TLR-3, which signals through TRIF adaptor protein (Ives et al., 2011). To investigate whether LRV1 promotes miR-155 expression through the TLR-3/TRIF signaling pathway, BMMs derived from WT, *TLR3*$^{-/-}$, and TRIF$^{\Delta LPS2}$ were infected with LRV1+ L.g or LRV1 − L.g. Poly I:C treatment was used as a positive control. Both LRV1 and poly I:C-induced miR-155 expression required functional TLR-3 and TRIF molecules, since the ablation of either TLR-3 or TRIF abrogated miR-155 expression (Figure 1F). These data indicated that the TLR-3/TRIF signaling pathway initiated the expression of miR-155 upon sensing LRV1 or synthetic dsRNA.

LRV1-Mediated miR-155 Expression Confers Increased Parasite Burden and Severity of Pathology in Mice

The role of miR-155 in the development of disease pathology was evaluated in vivo by infecting both WT and *miR-155*$^{-/-}$ mice in the footpad. A drastic decrease in footpad

swelling and reduced parasite burden at the peak of infection was observed in *miR-155*$^{-/-}$ mice infected with LRV1+ L.g (Figures 2A and 2B). In the case of LRV1 − L.g infection, no significant difference in disease pathology was detected between WT and *miR-155*$^{-/-}$ mice (Figures 2A and 2B). These findings suggested that LRV1-mediated host miR-155 expression played a crucial role in the survival of LRV1+ L.g parasites in mice.

Since miR-155 has also been shown to be required for the normal function of B cells and antibody secretion (Rodriguez et al., 2007; Thai et al., 2007), we decided to determine the impact of B cells on L.g infection. WT mice and mice lacking mature B cells (*Jh*$^{-/-}$) were infected with LRV1+ L.g. Infected WT and B cell-deficient mice displayed similar footpad swelling and parasitemia profiles (Figures S1A and S1B). We additionally examined B cell responses of miR-155-deficient mice infected with LRV1+ L.g by measuring total serum anti-LRV1 capsid immunoglobulin G (IgG) titers. Infected *miR-155*$^{-/-}$ mice produced reduced titers of anti-LRV1 capsid IgG compared to infected WT mice (Figure S1C). These data suggested that B cells and the antibody response were not involved in the pathology of *Leishmania* infection, and were not essential for the LRV1+ L.g parasite resistant phenotype of *miR-155*$^{-/-}$ mice.

It has also been reported that in in vitro differentiation conditions, CD4^{+} T cells lacking miR-155 secrete more IL-4 than WT CD4^{+} T cells, but similar levels of IFN-γ (Rodriguez et al., 2007). IFN-γ, which is predominantly secreted by CD4^{+} T cells, augments macrophage parasiticidal activity, while IL-4 suppresses it (Sacks and Sher, 2002). Therefore, we evaluated the role of CD4^{+} T cells, which are required for controlling *Leishmania* parasites in our model of infection. To determine the impact of miR-155 on IL-4- and IFN-γ-secreting CD4^{+} T cells during L.g infection, at the peak of infection we used intracellular flow cytometry analysis on the popliteal lymph node cells from WT and *miR-155*$^{-/-}$ mice infected either with LRV1+ L.g or LRV1 − L.g. Our results showed that the number and percentages of IFN-γ- and IL-4-secreting CD4^{+} T cells in LRV1+ L.g-infected mice were similar to those found in LRV1 − L.g-infected mice (Figures 2C and S2). These data indicated that the reduced disease progression in *miR-155*$^{-/-}$ mice in response to LRV1+L.g did not arise from an IFN-γ/IL-4 imbalance.

To further investigate the role of T cells in LRV1+ L.g infection, WT and *miR-155*$^{-/-}$ mice were injected with anti-CD4-depleting antibody 5 days prior to infection and on a weekly basis until 6 weeks post-infection (Figure S3A). We verified the efficiency of the antibody-mediated depletion using flow cytometry (Figures S3B and S3C). Interestingly, CD4 depletion caused a significant decrease in footpad swelling at 2–3 weeks post-infection in both LRV1+ L.g-infected WT and *miR-155*$^{-/-}$ mice (Figure 2D). We also observed that the resolution of footpad swelling was impaired in both LRV1+ L.g-infected WT and *miR-155*$^{-/-}$ mice after week 5 (Figure 2D). These data indicated that CD4^{+} cells contributed to lesion development early in LRV1+ L.g infection in a miR-155-independent manner and were required for the LRV1+ L.g infection resolution.

We analyzed parasite load in CD4-depleted WT and *miR-155*$^{-/-}$ mice infected with LRV1+ L.g. We found that CD4 depletion had no effect on parasite burden in WT mice, but led to a significant increase in parasite load at the peak of infection in LRV1+ L.g-infected

miR-155$^{-/-}$ mice (Figure 2E). These data suggested that CD4^{+} T cells were required for control of LRV1+ L.g during the earlier phases of infection in *miR-155*$^{-/-}$ mice, but not in WT mice, which probably have a compensatory source of IFN-γ other than CD4^{+} T cells in this time frame.

To better understand the possible impact of IFN-γ on the resistant phenotype of *miR-155*$^{-/-}$ mice against LRV1+ L.g infection, we crossed *miR-155*$^{-/-}$ mice with mice lacking IFN-γ to generate IFN-γ xmiR-155 double-knockout (DKO) mice. We then infected these mice with LRV1+ L.g parasites. Our data showed that the lesion size of infected *IFN-γ*$^{-/-}$ and DKO mice was similar, and was greater than that of their IFN-γ sufficient counterparts (Figure 2F). These findings showed that IFN-γ is essential for the clearance of L.g both in WT and *miR-155*$^{-/-}$ mice.

Macrophages Lacking miR-155 Do Not Exhibit Any Changes in the LRV1-Mediated Hyper-inflammatory Response

TLR-3 recognition of LRV1 induces a hyper-inflammatory response in macrophages, leading to the secretion of pro-inflammatory cytokines and an increase in infection severity in mice (Ives et al., 2011). We thus tested whether a deficiency in miR-155 expression could affect the LRV1-mediated pro-inflammatory cytokine profile in macrophages. BMMs were treated with poly I:C or infected with either LRV1+ L.g or LRV1 − L.g. The supernatants were assayed for IL-6 and TNF-α. As shown previously, WT BMMs secreted IL-6 and TNF-α after 24 hr in the presence of poly I:C or LRV1+ L.g (Figure 3A). The TLR-3 activation of *miR-155*$^{-/-}$ BMMs yielded similar cytokine profiles to those found in WT macrophages, providing evidence that miR-155 did not play a role in the inflammatory response to LRV1.

We subsequently evaluated whether miR-155 deficiency had an impact on IRF3 activation, which in turn could lead to a decrease in the mRNA and protein level of IFN-β. WT BMMs, along with macrophages deficient in miR-155 or TLR3, were treated with poly I:C or infected with either LRV1+ L.g or LRV1 − L.g. We observed that in the presence of LRV1+ L.g or poly I:C, IRF-3 phosphorylation occurred as early as 2 hr following stimulation and became undetectable after 6 hr (Figure 3B). To compare the IRF3 phosphorylation levels between WT, *TLR3*$^{-/-}$, and *miR-155*$^{-/-}$ in response to infection, the cells were lysed 2 hr following infection. A change was not observed in IRF-3 phosphorylation in response to LRV1+ L.g infection or poly I:C between WT and *miR-155*$^{-/-}$ BMMs (Figure 3C). As expected, the phosphorylated form of IRF-3 was undetectable under all conditions in *TLR3*$^{-/-}$ -infected macrophages (Figure 3C). Consistent with these findings, IFN-β was not significantly different between LRV1+ L.g-infected WT and *miR-155*$^{-/-}$ macrophages at either the transcriptional or the protein level (Figures 3D and 3E). These data ruled out the hypothesis that the absence of miR-155 could decrease the hyper-inflammatory responses arising from the innate sensing of LRV1.

LRV1+ L.g Infection Promotes Activation of the PI3K/Akt Signaling Pathway

The infection of macrophages with *Leishmania* parasites activates the PI3K/Akt signaling pathway (Ruhland et al., 2007), which is regulated, in part, by miR-155 in TLR-stimulated

macrophages (O'Connell et al., 2009). We thus asked whether the infection of macrophages with LRV1+ L.g or LRV1 − L.g promoted activation of Akt via miR-155. We analyzed Akt and its targets by immunodetection in cell lysates of BMMs that were incubated with medium, poly I:C, LRV1+ L.g, or LRV1 − L.g. At 2 hr post-infection, the phosphorylation of Akt was increased in all conditions except in the medium-treated cells. Phosphorylated Akt levels in LRV1 − L.g-infected macrophages were reduced after 6 hr, but were still evident after 10 hr in both LRV1+ L.g infection and poly I:C stimulation. Corresponding to these results, the level of pro-apoptotic Foxo3a gradually decreased in macrophages incubated with LRV1+ L.g or poly I:C, in accordance with a pro-survival effect of AKT (Litvak et al., 2012). We observed that the phosphorylation of GSK3-β was substantially greater in the presence of LRV1 or poly I:C at 6 hr post-infection than in LRV1 − L.g infection (Figure 4A). We also detected an increase in mTOR and S6K phosphorylation in WT macrophages incubated with LRV1+ L.g, LRV1 − L.g, or poly I:C for 2 hr (Figure 4A). Comparatively, we found higher levels of phosphorylated mTOR and S6K in macrophages incubated with LRV1+ L.g and poly I:C for 6 and 10 hr (Figure 4A). Notably, we showed that LRV1- or poly-I:C-mediated Akt activation in macrophages could be abrogated upon pre-treatment with either the Akt inhibitor MK2206 or the PI3K inhibitor wortmanin (Figure S4). Thus, L.g infection of macrophages promoted activation of the Akt-dependent pro-survival signaling pathway, and this activation was intensified and prolonged in the presence of LRV1.

Since LRV1+ L.g infection elicited an increase in Akt phosphorylation in macrophages 10 hr post-infection, we investigated the role of miR-155 and TLR-3 in LRV1-mediated Akt activation. Protein levels of phosphorylated Akt and its targets were evaluated in WT, *miR-155*$^{-/-}$, and *TLR3*$^{-/-}$ macrophage lysates at 10 hr post-infection. It was observed that LRV1-mediated Akt activation and Akt-dependent modulation of targets relied on TLR-3, and that miR-155 was partly involved in LRV1-mediated Akt activation (Figures 4B and 4C). Since miR-155 deficiency in TLR-stimulated macrophages results in an approximately 1.5-fold increase in the protein levels of the Src homology 2 domain-containing inositol-5-phosphatase 1 (SHIP1), a negative regulator of the PI3K/Akt signaling pathway (O'Connell et al., 2009), we investigated the changes in the SHIP1 protein level in WT, *miR-155*$^{-/-}$, and *TLR3*$^{-/-}$ macrophages in response to LRV1 at 24 hr post-infection. As previously reported, we observed a 1.5-fold increase in the protein level of SHIP1 in LRV1+ L.g-infected miR-155-deficient macrophages over their WT counterparts (Figure S5A and S5B), indicating that LRV1-mediated miR-155 expression could induce Akt activation by modulating SHIP1 protein levels.

To determine whether miR-155 contributed to Akt activation in infected animals, we performed flow cytometry analysis to measure phosphorylated Akt levels in lesional macrophages from LRV1+ L.g or LRV1 − L.g-infected WT and *miR-155*$^{-/-}$-infected mice at 4 weeks post-infection (Figure S6). We found that lesional macrophages from infected *miR-155*$^{-/-}$ mice displayed a significant reduction in phosphorylated Akt levels compared to WT infected mice (Figure 4D), whereas no significant difference was observed in LRV − L.g-infected WT or *miR-155*$^{-/-}$ mice. Taken together, our results indicated that miR-155 was involved in the TLR-3 mediated activation of the pro-survival PI3K/Akt signaling pathway in macrophages infected with LRV1+ L.g.

TLR-3-Mediated Cell Survival Is Dependent on TLR Ligand Concentration and Akt Activation

Studies using knockout animal models have shown that *Leishmania* molecules interact with several TLRs; however, current knowledge on the identity and function of these molecules and their cognate TLRs is limited (Ives et al., 2014). Our results demonstrated that LRV1 drastically enhanced the L.g-mediated activation of the pro-survival signaling pathway Akt, suggesting that the innate recognition of L.g through other TLRs could induce the activation of Akt. Thus, we raised the question of how TLR-mediated Akt activation affected the cellular fitness of macrophages in terms of cell survival. To this end, we performed high-content microscope analysis of WT and *miR-155*$^{-/-}$ macrophages pretreated with DMSO or the allosteric Akt inhibitor MK2206. We then incubated the macrophages with various TLR- and nucleotide-binding oligomerization domain-containing protein (NOD) ligands for 48 hr. We found that the ligation of certain TLRs, such as TLR-1/2 and TLR-5, did not promote cell survival (Figures 5A and 5B). In contrast, TLR-2/6, TLR-4, and TLR-7 ligation promoted macrophage survival. This effect was not, however, diminished by MK2206 pre-treatment at higher concentrations of TLR ligand (Figures 5A and 5B). TLR-3 binding induced cell survival in a dose- and Akt-dependent manner, while Akt-dependent cell survival in the presence of TLR-2 and TLR-9 ligands was only observed at the highest agonist concentration. The fold change in WT macrophage numbers was similar to the fold change in miR-155 macrophage numbers in all conditions, except in macrophages treated with the TLR-9 ligand ODN 2006 (Figures 5A and 5B). Taken together, these findings showed that the engagement of certain TLRs promoted macrophage survival in an Akt-dependent or -independent manner and that this effect varied depending on the TLR-ligand concentration.

LRV1+ L.g-Induced Macrophage Survival through the TLR-3/Akt Axis Is Partially Dependent on miR-155

Our results demonstrated that TLR-3 stimulation promoted macrophage survival through the Akt signaling pathway. To determine whether LRV1-mediated Akt activation promoted parasite persistence by inducing macrophage survival through miR-155 or TLR-3, BMMs were pre-incubated with DMSO or MK2206 and then infected with a multiplicity of infection (MOI) of 1 of L.g parasites either containing LRV1 or not. We found that the infection of WT and *miR-155*$^{-/-}$ macrophages with 1 MOI of LRV1+ L.g increased macrophage survival. This effect was reversed by MK2206 pre-treatment in WT BMMs, but not in *miR-155*$^{-/-}$ and *TLR-3*$^{-/-}$ BMMs (Figures 6A and 6B). Confirming our previous work (Zangger et al., 2014), the presence of LRV1 within parasites did not affect the parasite number per macrophage, but did affect infected macrophage survival (Figure 6C). Taken together, these results indicated that LRV1 dsRNA genome ligation to TLR-3 promoted macrophage survival, and therefore parasite persistence, by activating the Akt signaling pathway in a partially miR-155-dependent manner.

DISCUSSION

Our results demonstrated that LRV1 was able to exploit the TLR-3/miR-155/Akt signaling axis to enhance macrophage survival and persistence of intracellular *Leishmania* parasites.

Interestingly, the miR-155/Akt signaling pathway is known to cause myeloid proliferative disorder in both humans and mice (O'Connell et al., 2008; Xue et al., 2014). However, a deficiency in the myeloid compartment is not observed in *miR-155*$^{-/-}$ mice under basal conditions (Rodriguez et al., 2007), suggesting that miR-155 function requires induction. It is known that miR-155 is the only microRNA upregulated upon TLR-3 ligation in macrophages, and also that other TLR receptor agonists also promote miR-155 expression (O'Connell et al., 2007). Concurrently, we found that miR-155 was the only microRNA among 1,179 miR-NAs which was significantly upregulated in the presence of LRV1 in a TLR-3/TRIF-dependent manner. We observed that LRV1 − L.g infection only weakly induced miR-155 and *BIC* expression, suggesting that the innate recognition of parasites promoted only a slight increase in miR-155 expression through PRRs other than TLR-3. We found that mice which were deficient in miR-155 had significantly reduced disease pathology when infected with LRV1+ L.g, but not when infected with LRV1 − L.g. These results indicated that LRV1 used host miR-155 as a persistence mechanism, a situation evocative of certain herpes-viruses which exert their virulence via the pathogenic overexpression of miR-155 from either viral or host origin (Gottwein et al., 2007; Linnstaedt et al., 2010; Zhao et al., 2011). In this regard, whether other protozoan parasites containing viruses belonging to the *Totiviridae* family can subvert the host immune system through TLR-3/miR-155 remains to be determined.

MiR-155 deficiency in mice was shown to be protective against T cell- and B cell-driven autoimmune disorders such as rheumatoid arthritis (Blüml et al., 2011; Kurowska-Stolarska et al., 2011), experimental autoimmune encephalomyelitis (O'Connell et al., 2010), and systemic lupus erythematous (Thai et al., 2013). Interestingly, however, in serum or autoantibody transfer arthritis models, which are predominantly driven by innate cells, the severity of joint inflammation is not different between WT and *miR-155*$^{-/-}$ mice (Blüml et al., 2011; Kurowska-Stolarska et al., 2011). In addition, WT and *miR-155*$^{-/-}$ macrophages secrete similar levels of TNF-α after in vitro stimulation with auto-antibody immune complexes (Kurowska-Stolarska et al., 2011). Other studies show that miR-155 impacts the pro-inflammatory cytokine profile of LPS-stimulated macrophages (Androulidaki et al., 2009) and other cell types (Tili et al., 2007) at the protein level by transfecting a microRNA mimic or antagonist. However, we did not observe a difference in the pro-inflammatory cytokine profile between WT and *miR-155*$^{-/-}$ primary murine macrophages in response to poly I:C or LRV1+L.g infection, either in terms of the secretion of pro-inflammatory cytokines (TNF-α, IL-6, and IFN-β), the expression of IFN-β mRNA, or the phosphorylation of IRF-3. These results might be explained by the difference in stimuli, but it should be noted that transfecting either microRNA mimics or antagonists could cause an increase in the expression of endogenous microRNA targets due to the overexpression-mediated saturation of the intracellular protein complex which guides microRNAs to their target mRNA (Khan et al., 2009).

We found that the IFN-γ- and IL-4-secreting CD4^{+} T cell numbers in LRV1+ L.g-infected WT mice were not different from LRV1+ L.g-infected *miR-155*$^{-/-}$ mice at the peak of infection, although it was previously shown that CD4^{+} T cells of miR-155-deficient mice secrete more IL-4 and similar levels of IFN-βunder in vitro differentiation conditions (Rodriguez et al., 2007). However, the IFN-γ and/or IL-4 secretion of ex vivo WT and

miR-155 $CD4^+$ T cells was found to be similar in different biological settings (Kurowska-Stolarska et al., 2011; O'Connell et al., 2010), suggesting that miR-155 affects $CD4^+$ T cell plasticity in a condition-specific manner. Interestingly, we showed that $CD4^+$ cells mediated footpad swelling in mice infected with LRV1+ L.g through miR-155-independent mechanisms. Thus, further studies are required to understand the role of $CD4^+$ T cell lineages in this miR155-independent LRV1-mediated disease pathology.

We demonstrated that *miR-155*$^{-/-}$ mice, unlike WT mice, required $CD4^+$ T cells to control parasite growth in the early phases of infection. Further, it is known that miR-155 deficiency impairs the effector function of other-IFN-γ-producing cells, such as NK cells (Trotta et al., 2012), which can play a compensatory role in the restriction of parasite growth in the absence of $CD4^+$ T cells in the early phases of infection (Scharton and Scott, 1993). In our study, we found that both WT and *miR-155*$^{-/-}$ mice were unable to control LRV1+ L.g infection in the absence of IFN-γ mediated immune pressure, suggesting that IFN-γ is absolutely essential to infection control in both WT and *miR-155*$^{-/-}$ mice.

Several reports have proposed that the infection of macrophages with *Leishmania spp.* promotes parasite persistence by enhancing macrophage survival (Akarid et al., 2004; Moore and Matlashewski, 1994; Moore et al., 1994; Ruhland et al., 2007). Addressing the question on how the innate recognition of LRV1 modifies host cells to induce the survival of LRV1's microbial host, we found that LRV1 induced the phosphorylation of the pro-survival protein kinase Akt through TLR-3 in a partially miR-155-dependent manner. Consistent with a previous study, our findings supported the observation that miR-155 can modulate the PI3K/Akt signaling pathway by regulating SHIP1 protein expression (O'Connell et al., 2009). Functionally, our data showed that neither the LRV1 status of L.g nor the deficiency of TLR-3 and miR-155 in macrophages had an impact on the number of parasites per macrophage in vitro. We cannot, however, exclude the involvement of TLR-3-expressing phagocytic cells, other than macrophages, which can act as host cells for *Leishmania* parasites, in the miR-155-deficiency-mediated protection against LRV1+ L.g infection in mice. Nonetheless, our findings revealed a virulence mechanism in LRV1+ L.g infection whereby LRV1 conferred a survival advantage to its parasite host by promoting the survival of infected macrophages, which are the definitive host cells for *Leishmania*, through a TLR3/miR-155/Akt signaling circuit. These results highlighted the potential clinical importance of oncogenic kinases during leishmaniasis, and identified several potential therapeutic targets to treat and prevent the disfiguring complications of cutaneous leishmaniasis.

EXPERIMENTAL PROCEDURES

Animals

All animal protocols described in this report were approved by the Swiss Federal Veterinary Office (SFVO), under the authorization numbers 2113.1 and 2113.2. Animal handling and experimental procedures were undertaken with strict adherence to the ethical guidelines set out by the SFVO and under inspection by the Department of Security and Environment of the State of Vaud, Switzerland. Details are given in the Supplemental Experimental Procedures.

Parasite Culture

Parasites were cultured at 26°C in complete Schneider's medium with L-glutamine (Sigma-Aldrich) and were supplemented with 1% penicillin/streptomycin (Amimed) and 20% fetal calf serum (FCS) (PAA). The parasites were passaged in culture for not more than five passages and isolated from mouse footpads to maintain their virulence. Details are given in the Supplemental Experimental Procedures.

Macrophage Infection

The femurs and tibias of naive mice were washed with medium containing 1% P/S to extract cells, which were differentiated into BMMs for 6 days using complete DMEM supplemented with L-929-conditioned media (EACC cell line, Sigma-Aldrich) at 37°C. BMMs were seeded on culture plates and incubated overnight. BMMs were infected with stationary-phase LRV1+ or LRV1 − L.g at MOI of 10 parasite per macrophage unless otherwise indicated. BMMs were also treated with poly I:C (Invivogen) at 2 μg/ml or pretreated with DMSO (Sigma-Aldrich) or 5 μM MK2206 (Apexbio) for 1 hr.

MicroRNA Microarray

Four independent experiments were performed. In each experiment, macrophages derived from two individual C57BL/6 mice were infected with LRV1+ or LRV1 − L.g, or lysed with RNAzol RT (Mrcgene) after 10 hr post-infection. As a control, macrophages were treated with medium or poly I:C for post-array verification by RT-PCR. Total RNA was isolated from samples, and microRNA microarray (Agilent mouse miRbase v18.0) was performed following the manufacturer's instructions. Details are given in the Supplemental Experimental Procedures.

The Quantification of MicroRNA and mRNA Using Quantitative Real-Time PCR

The miR-16 and miR-155 levels were quantified with stem-loop RT-PCR. The abundance of mRNA and pre-miRNA was quantified with RT-PCR using Taqman probe or SYBR-Green-based (Roche) detection. The results were normalized against 60S ribosomal protein L32 (L32) for mRNA and miR-16 for microRNA. Details are given in the Supplemental Experimental Procedures.

Mice Infection and the Quantification of Parasite Burden by Bioluminescence

Age-matched mice were infected with 1×10^6 stationary *Leishmania* parasites in both hind footpads. Change in footpad thickness was monitored on a weekly basis. As described previously (Ives et al., 2011), parasite burden was quantified in mice by intra-peritoneally injecting D-Luciferin sodium salt (Regis Technologies) in 1× PBS at a concentration of 150 mg/kg. The images were acquired and analyzed using a Xenogen Lumina II imaging system (IVIS) and Living Image software. Mice were anesthetized with isoflurane during image acquisition. Oval regions of interest (ROI) were set on the footpads and the tail to determine the parasite burden and the background, respectively. Bioluminescent signals were expressed in units of photons per second (P/s).

Flow Cytometry Analysis

Popliteal lymph nodes (PLNs) or footpad lesions (FLs) were harvested from infected mice at the peak of infection. A single-cell suspension was prepared from FLs and PLNs with or without collagenase and DNaseI treatment, respectively. Cells isolated from PLNs were counted before PMA and ionomycin in vitro stimulation. Extracellular staining was performed using anti-mouse CD4 and CD8 antibodies. Cells were intracellularly stained for IFN-γ and IL-4 cytokines using an intracellular fixation and permeabilization buffer set, following the manufacturer's instructions (eBioscience). Cells isolated from FLs were fixed and permeabilized as described before (Krutzik and Nolan, 2003), and subsequently stained with CD45, CD11b, CD11c, F4/80, and p-Akt (T308) antibodies. Samples were acquired in BD FACSVerse or LSR II flow cytometry and were analyzed using FlowJo software. Details are given in the Supplemental Experimental Procedures.

In Vivo Depletion of CD4 Cells

Anti-CD4 GK1.5 monoclonal antibody was purified from hybridoma (GK1.5; ATCC) culture supernatant using affinity chromatography on HiTrap Protein G columns (Amersham-Pharmacia). Mice were intraperitoneally injected with 500 μg anti-CD4 GK1.5 antibody 5 days prior to infection and on a weekly basis until 7 weeks post-infection. The splenocytes of mice were harvested to verify the efficiency of antibody-mediated depletion using flow cytometry.

The Quantification of Cytokine Concentration in In Vitro Culture

The concentrations of TNF-α (eBioscience), IL-6 (eBioscience), and IFN-β (PBL, Interferon Source) in collected supernatants from treated macrophages were determined using enzyme-linked immuno-sorbent assay (ELISA) following the manufacturer's instructions. The plates (Nunc-Immuno) were read on a Synergy HT Multi-Mode Plate Reader (Biotek Instruments). Wavelength correction and background signals were subtracted from the absorbance values.

Western Blot Analysis

Cells were lysed using cell lysis buffer containing protease/phoshotase inhibitors. Cell lysates were run on SDS-PAGE, transferred to nitrocellulose membrane, and analyzed by western blotting using antibodies specific for the indicated antigens. Details are given in the Supplemental Experimental Procedures.

High-Content Microscopy

BMMs were counted with Vi-Cell (Beckman Coulter), then seeded on 96-well tissue-culture-treated clear-bottom plates (Falcon). After overnight incubation, cells were treated with DMSO (Sigma-Aldrich) or 5 μM MK2206 (ApeXBio) for 1 hr. Subsequent to a washing step, BMMs were treated with ligands in Multi-TLR array (Invivogen) medium, poly I:C (2 μg/ml), LRV1+ L.g, or LRV1 − L.g for 48 hr. Cells were fixed with freshly made 3.7% PFA in 1× PBS (pH 7.4), stained with DAPI (Molecular Probes) and Alexa 488-Phalloidin (Molecular Probes) then washed with 1× PBS using a Biotek MultioFlo FX plate washer. Forty-nine images (7 × 7 square, 0.12 mm^2) were acquired from each well using

ImageXpress Micro XLS. Cell and parasite numbers were counted using an automated software program (MetaExpress).

Statistical Analysis

All graphs were generated in GraphPad Prism. Unpaired Student's t tests and repeated-measure two-way ANOVA tests were performed using Microsoft Excel and GraphPad Prism, respectively. We considered $p < 0.05$ and $p < 0.001$ for unpaired Student's t test and repeated-measure two-way ANOVA test with Bonferroni's post test to be statistically significant, respectively. NS stands for a non-significant statistical difference. p values are shown as * for $p < 0.05$, ** for $p < 0.01$, and *** for $p < 0.001$.

Acknowledgments

We thank S. Hickerson and K. Owens for assistance with generation and handling of luciferase-expressing L.g. We thank K. Harshman and F.C. Barras (Center of Integrative Genomics, UNIL) for the microRNA microarray experiment. We thank D. Monreau and C.U. Eren for assistance with the high-content microscopy and S. Masina for critical reading of the manuscript. We thank the NCCR Geneva Access platform for providing the equipment for the high-content microscope experiments. This work is funded by grants from the Swiss National fund for research (FNRS 310030-153204 and IZRJZ3_164176, N.F.), the Institute for Arthritis Research (iAR), the COST action (CM1307 SE-FRI: C14.0070, N.F.), the Pierre Mercier Foundation (M.A.H. and C.R.), and the NIH (R56AI099364 and R01AI029646, S.M.B.).

References

Akarid K, Arnoult D, Micic-Polianski J, Sif J, Estaquier J, Ameisen JC. Leishmania major-mediated prevention of programmed cell death induction in infected macrophages is associated with the repression of mitochondrial release of cytochrome c. J Leukoc Biol. 2004; 76:95–103. [PubMed: 15075349]

Androulidaki A, Iliopoulos D, Arranz A, Doxaki C, Schworer S, Zacharioudaki V, Margioris AN, Tsichlis PN, Tsatsanis C. The kinase Akt1 controls macrophage response to lipopolysaccharide by regulating microRNAs. Immunity. 2009; 31:220–231. [PubMed: 19699171]

Blüml S, Bonelli M, Niederreiter B, Puchner A, Mayr G, Hayer S, Koenders MI, van den Berg WB, Smolen J, Redlich K. Essential role of microRNA-155 in the pathogenesis of autoimmune arthritis in mice. Arthritis Rheum. 2011; 63:1281–1288. [PubMed: 21321928]

Bogdan C, Röllinghoff M, Diefenbach A. Reactive oxygen and reactive nitrogen intermediates in innate and specific immunity. Curr Opin Immunol. 2000; 12:64–76. [PubMed: 10679404]

Cooray S. The pivotal role of phosphatidylinositol 3-kinase-Akt signal transduction in virus survival. J Gen Virol. 2004; 85:1065–1076. [PubMed: 15105524]

Gottwein E, Mukherjee N, Sachse C, Frenzel C, Majoros WH, Chi JT, Braich R, Manoharan M, Soutschek J, Ohler U, Cullen BR. A viral microRNA functions as an orthologue of cellular miR-155. Nature. 2007; 450:1096–1099. [PubMed: 18075594]

Heussler VT, Küenzi P, Rottenberg S. Inhibition of apoptosis by intracellular protozoan parasites. Int J Parasitol. 2001; 31:1166–1176. [PubMed: 11563357]

Hsu LC, Park JM, Zhang K, Luo JL, Maeda S, Kaufman RJ, Eckmann L, Guiney DG, Karin M. The protein kinase PKR is required for macrophage apoptosis after activation of Toll-like receptor 4. Nature. 2004; 428:341–345. [PubMed: 15029200]

Huang S, Houghton PJ. Targeting mTOR signaling for cancer therapy. Curr Opin Pharmacol. 2003; 3:371–377. [PubMed: 12901945]

Hurley J, Roberts D, Bond A, Keys D, Chen C. Stem-loop RT-qPCR for microRNA expression profiling. Methods Mol Biol. 2012; 822:33–52. [PubMed: 22144190]

Ives A, Ronet C, Prevel F, Ruzzante G, Fuertes-Marraco S, Schutz F, Zangger H, Revaz-Breton M, Lye LF, Hickerson SM, et al. Leishmania RNA virus controls the severity of mucocutaneous leishmaniasis. Science. 2011; 331:775–778. [PubMed: 21311023]

Ives A, Masina S, Castiglioni P, Prével F, Revaz-Breton M, Hartley MA, Launois P, Fasel N, Ronet C. MyD88 and TLR9 dependent immune responses mediate resistance to Leishmania guyanensis infections, irrespective of Leishmania RNA virus burden. PLoS ONE. 2014; 9:e96766. [PubMed: 24801628]

Iwasaki A, Medzhitov R. Toll-like receptor control of the adaptive immune responses. Nat Immunol. 2004; 5:987–995. [PubMed: 15454922]

Khan AA, Betel D, Miller ML, Sander C, Leslie CS, Marks DS. Transfection of small RNAs globally perturbs gene regulation by endogenous microRNAs. Nat Biotechnol. 2009; 27:549–555. [PubMed: 19465925]

Krutzik PO, Nolan GP. Intracellular phospho-protein staining techniques for flow cytometry: monitoring single cell signaling events. Cytometry A. 2003; 55:61–70. [PubMed: 14505311]

Kurowska-Stolarska M, Alivernini S, Ballantine LE, Asquith DL, Millar NL, Gilchrist DS, Reilly J, Ierna M, Fraser AR, Stolarski B, et al. MicroRNA-155 as a proinflammatory regulator in clinical and experimental arthritis. Proc Natl Acad Sci USA. 2011; 108:11193–11198. [PubMed: 21690378]

Linnstaedt SD, Gottwein E, Skalsky RL, Luftig MA, Cullen BR. Virally induced cellular microRNA miR-155 plays a key role in B-cell immortalization by Epstein-Barr virus. J Virol. 2010; 84:11670–11678. [PubMed: 20844043]

Litvak V, Ratushny AV, Lampano AE, Schmitz F, Huang AC, Raman A, Rust AG, Bergthaler A, Aitchison JD, Aderem A. A FOXO3-IRF7 gene regulatory circuit limits inflammatory sequelae of antiviral responses. Nature. 2012; 490:421–425. [PubMed: 22982991]

Lombardo E, Alvarez-Barrientos A, Maroto B, Boscá L, Knaus UG. TLR4-mediated survival of macrophages is MyD88 dependent and requires TNF-alpha autocrine signalling. J Immunol. 2007; 178:3731–3739. [PubMed: 17339471]

Moore KJ, Matlashewski G. Intracellular infection by Leishmania donovani inhibits macrophage apoptosis. J Immunol. 1994; 152:2930–2937. [PubMed: 8144893]

Moore KJ, Turco SJ, Matlashewski G. Leishmania donovani infection enhances macrophage viability in the absence of exogenous growth factor. J Leukoc Biol. 1994; 55:91–98. [PubMed: 8283144]

O'Connell RM, Taganov KD, Boldin MP, Cheng G, Baltimore D. MicroRNA-155 is induced during the macrophage inflammatory response. Proc Natl Acad Sci USA. 2007; 104:1604–1609. [PubMed: 17242365]

O'Connell RM, Rao DS, Chaudhuri AA, Boldin MP, Taganov KD, Nicoll J, Paquette RL, Baltimore D. Sustained expression of microRNA-155 in hematopoietic stem cells causes a myeloproliferative disorder. J Exp Med. 2008; 205:585–594. [PubMed: 18299402]

O'Connell RM, Chaudhuri AA, Rao DS, Baltimore D. Inositol phosphatase SHIP1 is a primary target of miR-155. Proc Natl Acad Sci USA. 2009; 106:7113–7118. [PubMed: 19359473]

O'Connell RM, Kahn D, Gibson WS, Round JL, Scholz RL, Chaudhuri AA, Kahn ME, Rao DS, Baltimore D. MicroRNA-155 promotes autoimmune inflammation by enhancing inflammatory T cell development. Immunity. 2010; 33:607–619. [PubMed: 20888269]

Park JM, Greten FR, Wong A, Westrick RJ, Arthur JS, Otsu K, Hoffmann A, Montminy M, Karin M. Signaling pathways and genes that inhibit pathogen-induced macrophage apoptosis–CREB and NF-kappaB as key regulators. Immunity. 2005; 23:319–329. [PubMed: 16169504]

Rakoff-Nahoum S, Medzhitov R. Toll-like receptors and cancer. Nat Rev Cancer. 2009; 9:57–63. [PubMed: 19052556]

Rodriguez A, Vigorito E, Clare S, Warren MV, Couttet P, Soond DR, van Dongen S, Grocock RJ, Das PP, Miska EA, et al. Requirement of bic/microRNA-155 for normal immune function. Science. 2007; 316:608–611. [PubMed: 17463290]

Ruhland A, Leal N, Kima PE. Leishmania promastigotes activate PI3K/Akt signalling to confer host cell resistance to apoptosis. Cell Microbiol. 2007; 9:84–96. [PubMed: 16889626]

Sacks D, Sher A. Evasion of innate immunity by parasitic protozoa. Nat Immunol. 2002; 3:1041–1047. [PubMed: 12407413]

Scharton TM, Scott P. Natural killer cells are a source of interferon gamma that drives differentiation of CD4+ T cell subsets and induces early resistance to Leishmania major in mice. J Exp Med. 1993; 178:567–577. [PubMed: 8101861]

Tam W. Identification and characterization of human BIC, a gene on chromosome 21 that encodes a noncoding RNA. Gene. 2001; 274:157–167. [PubMed: 11675008]

Thai TH, Calado DP, Casola S, Ansel KM, Xiao C, Xue Y, Murphy A, Frendewey D, Valenzuela D, Kutok JL, et al. Regulation of the germinal center response by microRNA-155. Science. 2007; 316:604–608. [PubMed: 17463289]

Thai TH, Patterson HC, Pham DH, Kis-Toth K, Kaminski DA, Tsokos GC. Deletion of microRNA-155 reduces autoantibody responses and alleviates lupus-like disease in the Fas(lpr) mouse. Proc Natl Acad Sci USA. 2013; 110:20194–20199. [PubMed: 24282294]

Tili E, Michaille JJ, Cimino A, Costinean S, Dumitru CD, Adair B, Fabbri M, Alder H, Liu CG, Calin GA, Croce CM. Modulation of miR-155 and miR-125b levels following lipopolysaccharide/TNF-alpha stimulation and their possible roles in regulating the response to endotoxin shock. J Immunol. 2007; 179:5082–5089. [PubMed: 17911593]

Trotta R, Chen L, Ciarlariello D, Josyula S, Mao C, Costinean S, Yu L, Butchar JP, Tridandapani S, Croce CM, Caligiuri MA. miR-155 regulates IFN-γ production in natural killer cells. Blood. 2012; 119:3478–3485. [PubMed: 22378844]

Valencia-Sanchez MA, Liu J, Hannon GJ, Parker R. Control of translation and mRNA degradation by miRNAs and siRNAs. Genes Dev. 2006; 20:515–524. [PubMed: 16510870]

Weichhart T, Hengstschläger M, Linke M. Regulation of innate immune cell function by mTOR. Nat Rev Immunol. 2015; 15:599–614. [PubMed: 26403194]

Xue H, Hua LM, Guo M, Luo JM. SHIP1 is targeted by miR-155 in acute myeloid leukemia. Oncol Rep. 2014; 32:2253–2259. [PubMed: 25175984]

Zangger H, Hailu A, Desponds C, Lye LF, Akopyants NS, Dobson DE, Ronet C, Ghalib H, Beverley SM, Fasel N. Leishmania aethiopica field isolates bearing an endosymbiontic dsRNA virus induce pro-inflammatory cytokine response. PLoS Negl Trop Dis. 2014; 8:e2836. [PubMed: 24762979]

Zhao Y, Xu H, Yao Y, Smith LP, Kgosana L, Green J, Petherbridge L, Baigent SJ, Nair V. Critical role of the virus-encoded microRNA-155 ortholog in the induction of Marek's disease lymphomas. PLoS Pathog. 2011; 7:e1001305. [PubMed: 21383974]

Highlights

- TLR-3 recognition of *Leishmania* RNA virus 1 (LRV1) induces miR-155 expression
- *MiR-155*$^{-/-}$ mice show a decrease in the pathogenesis of LRV1+ *Leishmania* infection
- LRV1 induces the activation of PI3K/Akt signaling through TLR-3 and miR-155
- LRV1 promotes parasite persistence by inducing host cell survival via Akt

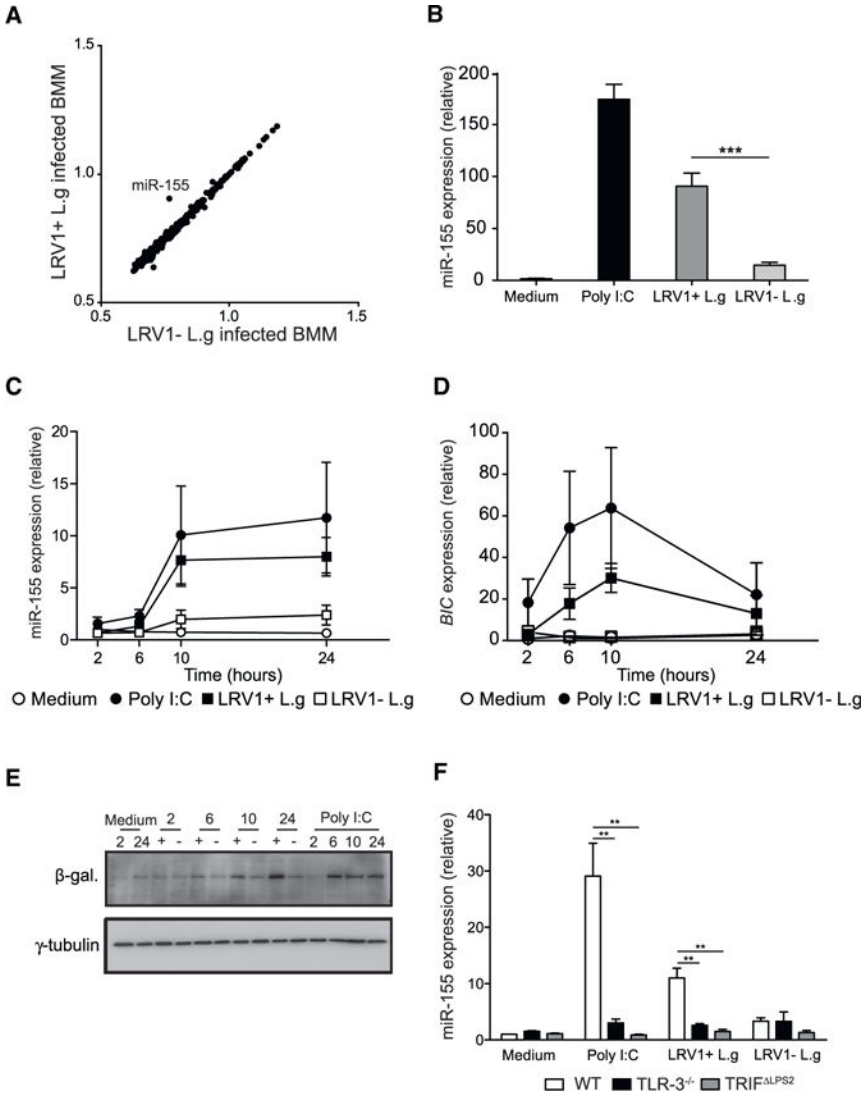

Figure 1. LRV1-Induced miR-155 Expression through TLR-3/TRIF Signaling

(A) MicroRNA microarray analysis was performed on total RNA extracted from WT BMMs infected with LRV1+ L.g and LRV1 − L.g for 10 hr. Scatter-plot shows $\log_{10}$-transformed normalized averaged intensity values (n = 4) for each miRNA probe.

(B) A portion of WT BMMs generated in (A) were treated with medium or poly I:C (2 μg/ml). RT-PCR was used to measure the abundance of the miR-155 in extracted RNA. The numbers represent relative miR-155 expression as fold induction over the medium-treated condition subsequent to normalization with miR-16. (C and D) Kinetic quantification of miR-16-normalized miR-155

(C) and L32-normalized *BIC*

(D) expression in WT BMMs incubated with medium, poly I:C (2 μg/ml), LRV1+ L.g, or LRV1 − L.g using RT-PCR.

(E) β-galactosidase western blot analysis of *miR-155*$^{-/-}$ BMMs infected with LRV1+ L.g (+) or LRV1 − L.g (−) at indicated time points. Cells treated with medium (as negative

control) or with poly I:C (2 μg/ml) (as positive control) were also blotted for β-galactosidase.

(F) The relative miR-155 expression levels of WT, *TLR-3*$^{-/-}$, and TRIF$^{\Delta LPS2}$ macrophages incubated with medium, poly I:C (2 βg/ml), LRV1+ L.g, or LRV1 − L.g.

Data are presented as mean ± SEM from the pool of three independent experiments (C, D, and F). Representative western blots were shown from three independent experiments (E). p values shown were calculated by unpaired Student's t test. **p < 0.01 and ***p < 0.001.

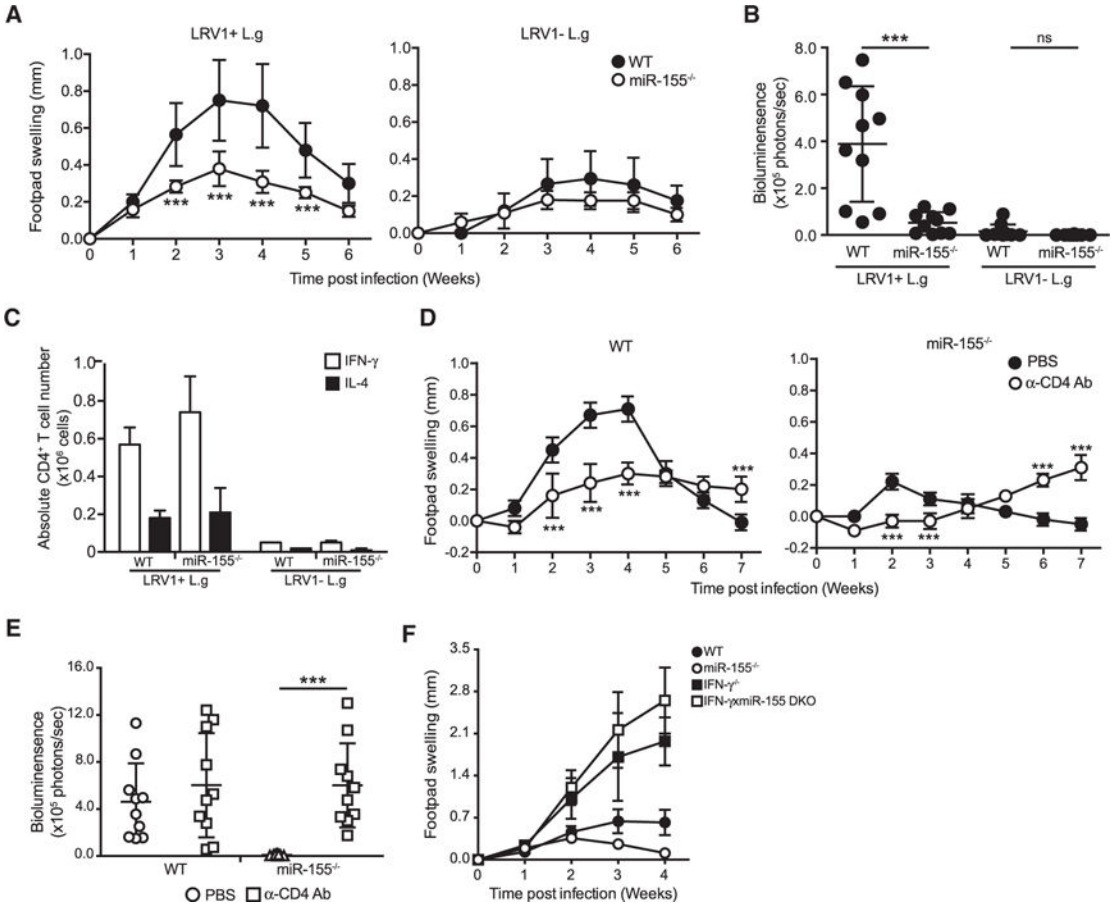

Figure 2. *MiR-155*$^{-/-}$ Mice Infected with LRV1+ L.g Parasites Had Decreased Disease Pathology when Compared to WT Mice

(A and B) Hind footpads of WT and *MiR-155*$^{-/-}$ mice were infected with 1 × 10^6 LRV1+ L.g or LRV1 − L.g.

(A) The graph displays the weekly measurement of footpad swelling.

(B) Parasite burden was determined at 3 weeks after infection by bioluminescence imaging.

(C) Popliteal lymph nodes were collected from WT and miR-155 mice infected with LRV1+ L.g or LRV1 − L.g on the footpad after 3 weeks of infection. Intracellular FACS analysis was performed using primary ex vivo lymphocytes extracted and stimulated with PMA/ionomycin to measure IL-4 and IFN-γ levels in $CD4^+$ T cells (see also Figure S2).

(D and E) Mice were intraperitoneally injected with CD4-depleting antibody 5 days prior to LRV1+ L.g infection and then on a weekly basis for 6 weeks. A group of mice was treated with PBS as a negative control (see also Figures S3 and S4).

(D) Footpad swelling of LRV1+ L.g-infected WT and *MiR-155*$^{-/-}$ mice.

(E) Parasite load was measured by bioluminescence 4 weeks post-infection.

(F) The measurement of footpad swelling in WT, *MiR-155*$^{-/-}$, IFN-γ, and IFN-γ xmiR-155 DKO mice following of LRV1+ L.g infection.

Data show mean ± SD from representative experiments (n = 4–5 mice) of two (C–E) or three (A, B, and F) independent experiments. Each dot in the scatter blot represents a footpad (B and E). Statistical significance is calculated using two-way ANOVA analysis with

Bonferonni's post test (A and D) and unpaired Student's t test (B and E). Not significant (NS), *$p < 0.05$, and ***$p < 0.001$. See also Figure S1.

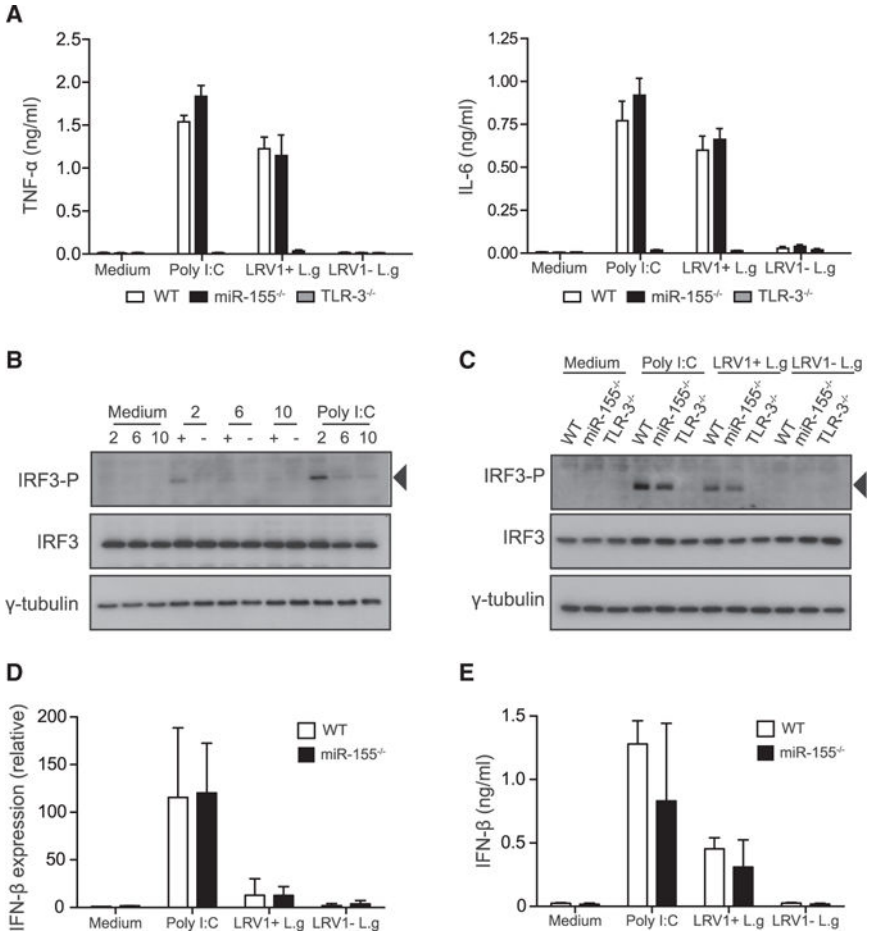

Figure 3. *MiR-155*$^{-/-}$ Macrophages Exhibited Similar Proinflammatory Cytokine Response Compared to WT Macrophages in Response to LRV1+ L.g or Poly I:C

(A–E) BMMs were infected with LRV1+ L.g (+) or LRV1 − L.g (). Cells were treated with medium or poly I:C (2 μg/ml) as a control for indicated times.

(A) The cell-free culture supernatant was collected 24 hr post-treatment from treated macrophages derived from WT, *TLR-3*$^{-/-}$, and *miR-155*$^{-/-}$ mice. These samples were assayed for IL-6 and TNF-α using ELISA.

(B) Total cell lysate of treated WT macrophages was analyzed by western blot with IRF3-P, IRF-3, and γ-tubulin after 2, 6, and 10 hr infection.

(C) WT, *TLR-3*$^{-/-}$, and *miR-155*$^{-/-}$ BMMs were lysed after 2 hr and immunoblotted for the indicated antibodies.

(D) IFN-β mRNA levels were assayed after 2 hr incubation using RT-PCR. Values were normalized using L32. Transcript levels were calculated relative to unstimulated WT macrophages.

(E) Protein level of IFN-β was quantified in collected cell culture medium after 6 hr treatment. Data are mean ± SD from three pooled independent experiments. Representative blots were shown from three independent experiments.

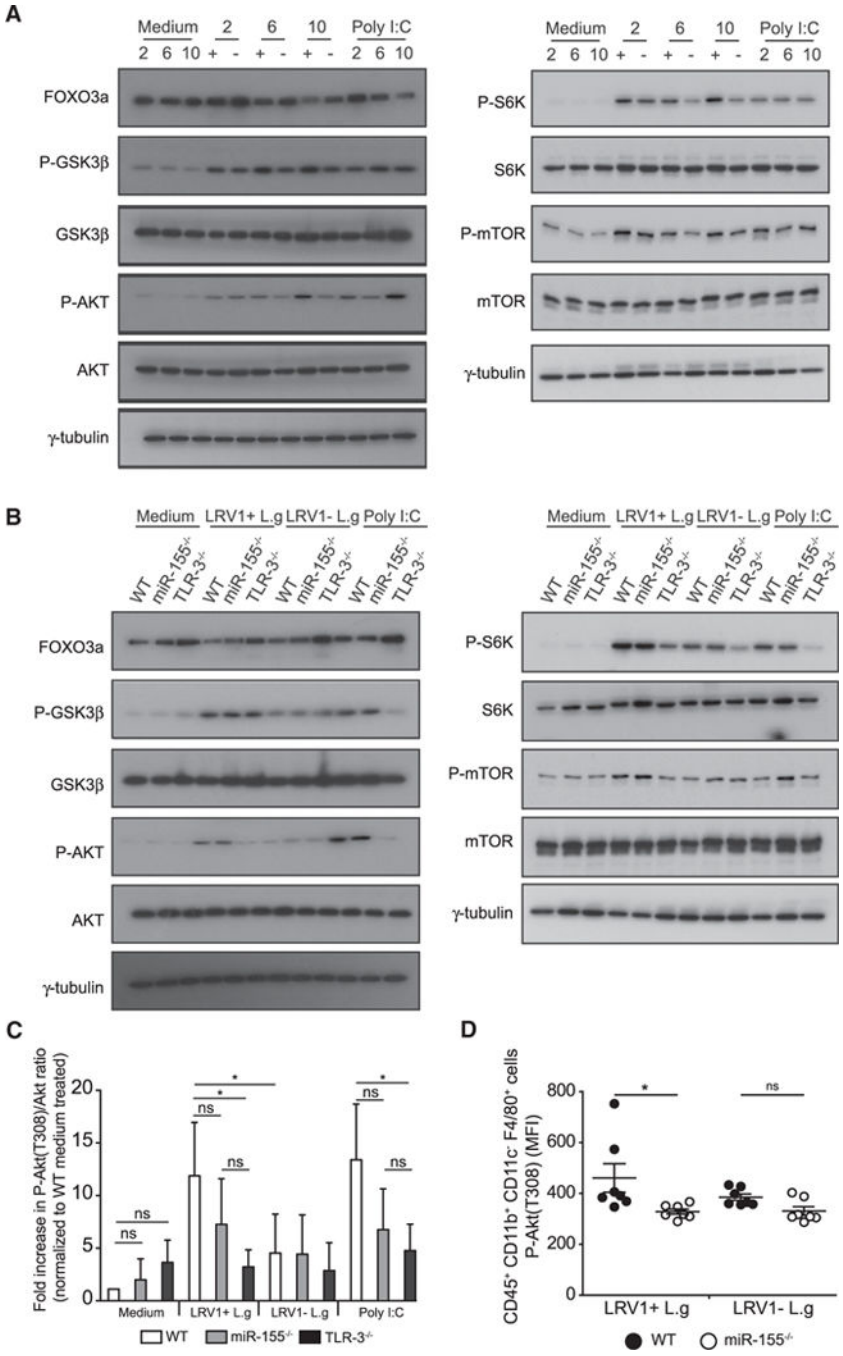

Figure 4. MiR-155 Partially Contributed to TLR-3-Dependent Akt Activation

(A and B) Macrophages incubated with medium, poly I:C, LRV1+ L.g (+), or LRV1 − L.g (−) for indicated time(s). Cells were lysed and total protein lysates were immunoblotted for Foxo3a, GSK3-β, phosho-GSK3-β (Ser9), Akt, phosho-Akt (T308), S6K, phosho-S6K (Thr389), mTOR, phosho-mTOR (Ser2448), and γ-tubulin.

(A) Whole-cell lysate of WT macrophages after 2, 6, and 10 hr post-treatment were immunoblotted for the indicated proteins.

(B) Macrophages derived from WT, *TLR-3*$^{-/-}$, and *miR-155*$^{-/-}$ mice were incubated with indicated conditions for 10 hr, and whole-cell lysates of indicated samples were subjected to western blot analysis with the indicated antibodies.

(C) Cell lysates described in (B) were immunoblotted for Akt, phosho-Akt (T308), and γ-tubulin. The levels of Akt (Thr308) phosphorylation were quantified by densitometric analysis. The data were normalized with total Akt and shown as fold increase of normalized Akt phosphorylation over the Akt (T308)/Akt ratio from medium-treated macrophages.

(D) Flow cytometry analysis of the mean fluorescence intensity (MFI) of phosphorylated Akt (T308) in $CD45^+$ $CD11b^+$ $CD11c^-$ $F4/80^+$ lesional macrophages from LRV1+ L.g- or LRV1 − L.g-infected WT and *miR-155*$^{-/-}$ mice at 4 weeks post-infection. See also Figure S6.

Representative blots (A–B) and quantification (C) from at least three independent experiments are shown. The graph (D) shows pooled data from two independent experiments (n = 2–5 mice). Data are expressed as mean ± SD. Unpaired Student's t test was used to measure statistical significance. Not significant (NS) and *$p < 0.05$. See also Figures S3 and S4.

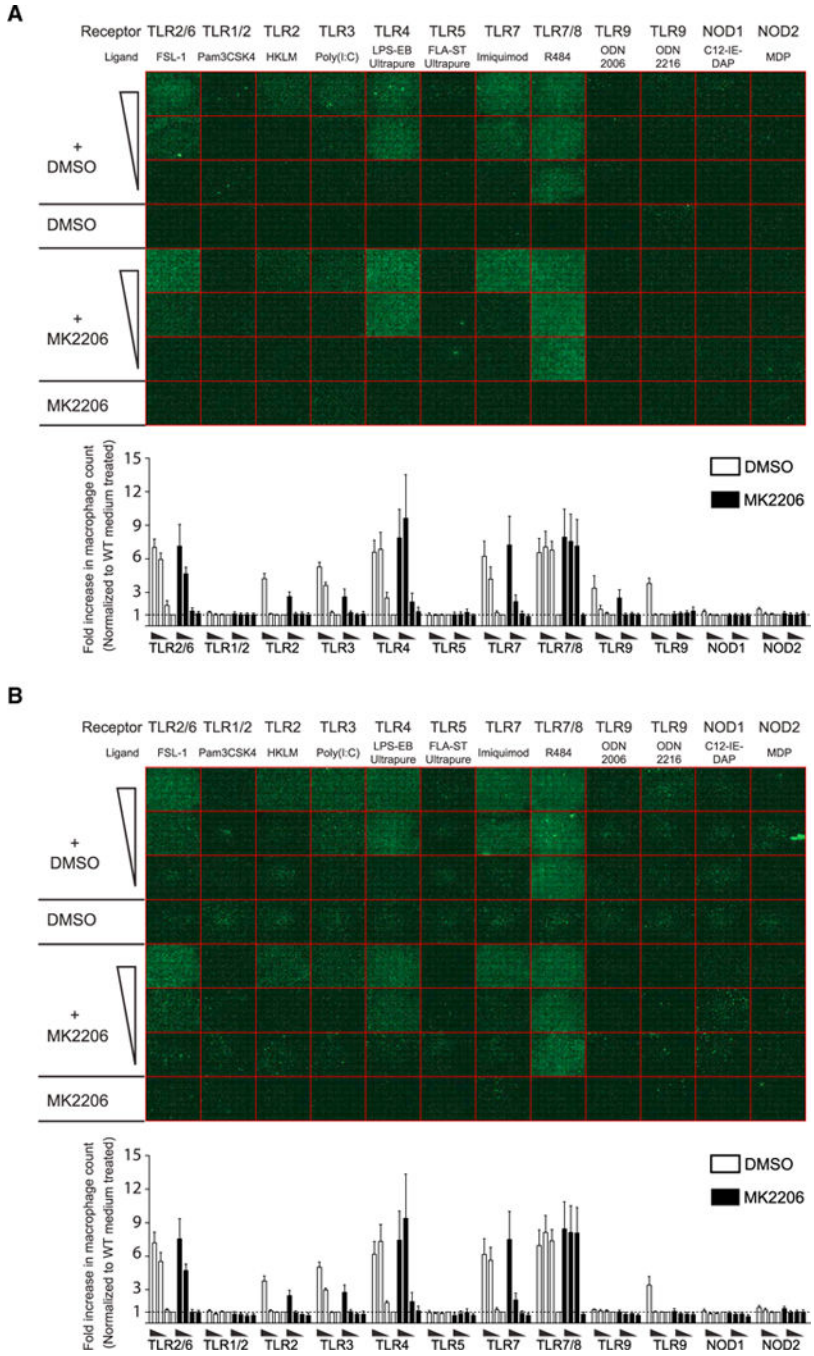

Figure 5. TLR-3-Induced Macrophage Survival in an Akt-Dependent Manner

(A and B) WT (A) and *miR-155*$^{-/-}$ (B) macrophages were seeded in 96-well plates and were pre-cultured with DMSO or MK2206 for 1 hr. Cells were treated with a series of three 10-fold dilutions of TLR ligands, and were fixed after 48 hr. Macrophages were stained with DAPI (nucleus) and phalloidin (cytoskeleton), and were analyzed with a high-content microscope. Images are in phalloidin channel and display an entire 96-well plate. Each square (352 μM × 352 μM) represents a well composed of 49 (7 × 7) pictures taken by 40×

lens. The fold increase in cell number was calculated by normalizing sample cell counts to the cell numbers within DMSO-treated wells.

Data represent mean ± SD from two independent experiments with three biological replicates. See also Table S1.

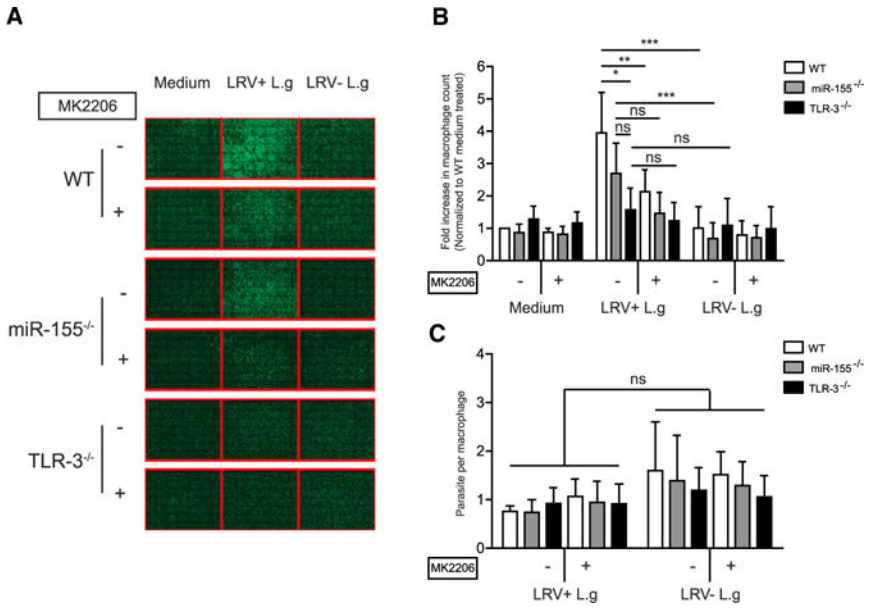

Figure 6. LRV1 Exploited the TLR-3/miR-155/Akt Pathway to Promote the Persistence of Its Microbial Host

(A–C) WT, *TLR-3*$^{-/-}$, and *miR-155*$^{-/-}$ macrophages were infected with promastigotes of LRV1+ or LRV1 − L.g at 1 MOI for 48 hr. Cells were fixed and processed for high-content analysis by staining with DAPI and phalloidin.

(A) A representative composite image of a well containing 7 × 7 pictures with 352 μM × 352 μM images from each condition were displayed in phalloidin channel.

(B) Relative macrophage number was quantified by normalizing cell numbers of the samples to the cell count of the medium-treated WT macrophages.

(C) Parasite load in macrophages described in (B) were quantified.

Mean ± SD was calculated from two independent experiments with three biological replicates in triplicate. Data were analyzed using unpaired Student's t test. Not significant (NS), *$p < 0.05$, **$p < 0.01$, and ***$p < 0.001$.